Low Energy Electron Cooler for NICA Booster

A.P. Denisov and V.V. Parkhomchuk
BINP, Novosibirsk, Russia

Abstract
BINP has developed an electron cooler to increase the ion accumulation efficiency in the NICA (Nuclotron-based Ion Collider fAcility) heavy ion booster (JINR, Dubna). Adjustment of the cooler magnetic system provides a highly homogeneous magnetic field in the cooling section $B_{trans}/B_{long} \leq 4 \cdot 10^{-5}$, which is vital for efficient electron cooling. First experiments with an electron beam performed at BINP demonstrated the target DC current of 500 mA and electron energy of 6 keV.

Keywords
NICA; booster; electron cooling; solenoid; magnetic field shape.

1 Introduction

1.1 NICA project

The main goal of the NICA project is to study the properties of dense baryonic matter including strong interaction and transition between baryonic matter and QGP (Quark-Gluon Plasma) [1]. This is studied in collisions of high-energy heavy ion beams; however, the most sophisticated part is to provide such beams. NICA Nuclotron will accelerate fully stripped ions up to an energy 4.5 GeV per nucleon, but since the Nuclotron is not able to strip ions by itself, a Booster will be added.

The NICA Booster will accumulate ions and accelerate them up to an energy, at which the ion stripping is the most efficient, and then send them to the Nuclotron. The Booster will include the low energy electron cooling system performing two main functions: to increase the ion accumulation efficiency and to cool the ion beam before stripping.

1.2 The electron cooler for the NICA Booster

The electron cooler will operate with ions at two different energies: an injection energy of 3.2 MeV per nucleon and an intermediate energy of 65 MeV per nucleon. The electron cooler for the NICA Booster provides an electron beam with energy ranging from 1.5 keV to 60 keV, which is necessary to match the energies of the electron and ion beams. More information about electron cooling can be found in [2]. The schematic layout of the cooler is shown in Fig. 1.

The most important part of the cooler is the cooling section. The quality of the magnetic fields in this section determines the efficiency of the cooling process. To achieve cooling times around one second the straightness of the magnetic field in the cooling section should be better than 10^{-5} rad. However, many factors such as assembly errors and magnetization of the magnetic elements affect the magnetic field straightness. These factors can change during the electron cooler operation, so one needs to compensate for them. Therefore, this article emphasises on the methods of magnetic measurements and adjustments of the magnetic system.

https://doi.org/10.23727/CERN-Proceedings-2017-001.135

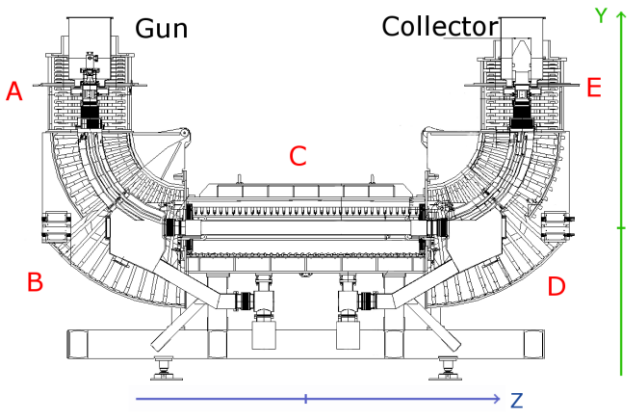

Fig. 1: The magnetic systemof the electron cooler. A,E – solenoids of gun and collector; B,D – bending magnets and dipoles; C – the cooling section including the main solenoid.

2 Magnetic measurements

Magnetic measurements discussed in this section include only measurements of magnetic field on the main solenoid axis. Two different measuring devices were used: Hall sensor and compass. The Hall sensor is widespread, so it is not described in this article. Using the Hall sensor, we measured magnetic fields along the cooling section created by each individual magnetic element, providing a rough estimate of their magnetization (Fig. 2). The compass is actually the magnetic needle, so it can measure the direction of magnetic field force lines with an accuracy about $10^{-6}\ rad$.

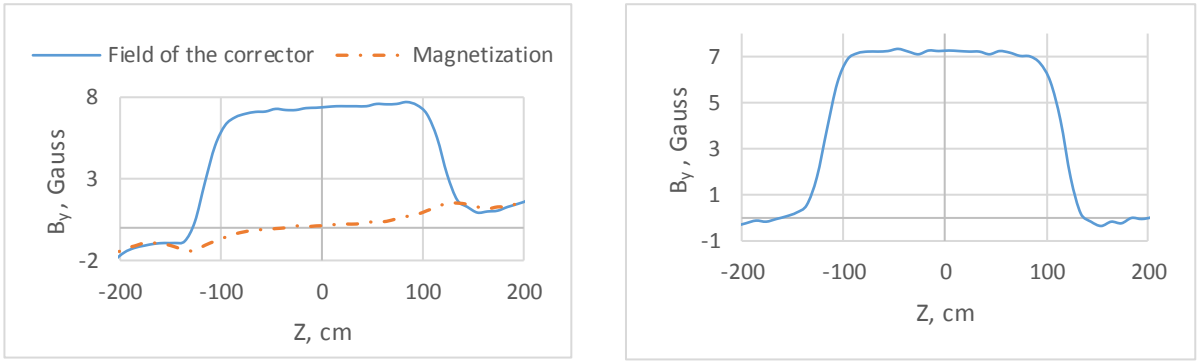

Fig. 2: Hall measurements of magnetic fields created by the vertical corrector in the cooling section. The graph on the left represents raw data, and on the right the processed response function of the corrector is shown. The corrector current is 5 A.

The scheme of magnetic measurements with the compass is shown in Fig. 3. The feedback system has laser optics whose optical axis aligns with the magnetic axis of the main solenoid. A laser beam propagates along the optical axis and reflects from a mirror placed on the compass. The reflected beam reaches a photo sensor that measures the displacement of the laser beam. In the presence of a transversal magnetic field in the cooling section, the compass is tilted from the solenoid axis. While it is tilted, the feedback system controls a compensating transverse magnetic field created by special coils placed near the compass to set the tilt of the compass to zero. By performing measurements with the compass along the cooling section the profile of the transverse magnetic field is measured.

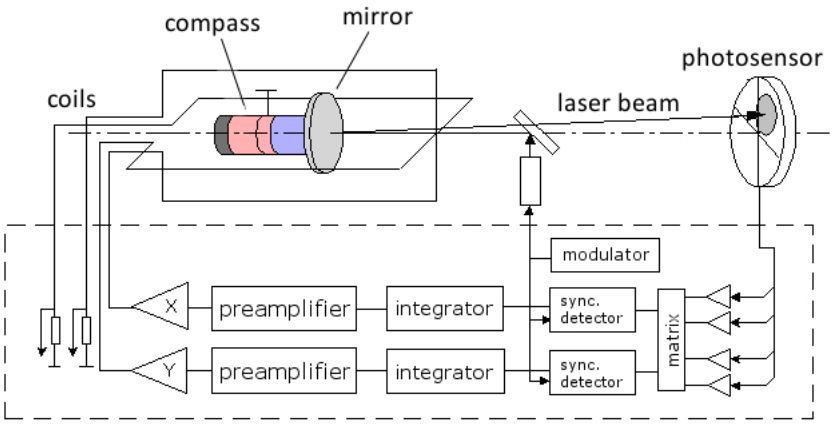

Fig. 3: The principal scheme of compass measurements

The ideal situation for the electron cooling is when there is no transverse magnetic field in the cooling section. However, due to assembly errors in magnetic elements and magnetization, the real magnetic profiles are always non-zero. In order to control the shape of the magnetic profiles the magnetic system of the electron cooler includes special correctors. Those correctors and methods of compensation of transverse magnetic fields are discussed in the next sections.

3 Magnetic field straightness

As noted in section 2, the magnetic profiles are always non-zero due to such factors as magnetization and solenoid assembly errors. However, these profiles can be corrected by using a special construction of the main solenoid.

The main solenoid consists of many independent coils, each of which can slightly rotate from its original position (Fig. 4). As a rotated coil contributes to the transverse magnetic profile, the right combination of coil rotations can reduce the magnetic profiles to zero.

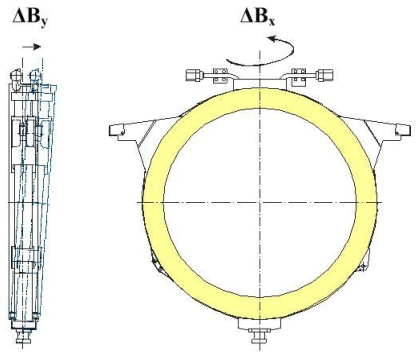

Fig. 4: One coil of the main solenoid. Moving the two upper handles, the coil can be rotated with respect to its pivot point, located at the bottom of the coil.

The procedure of compensation includes several steps. The initial profile is measured. Subsequently a correction to the position of one of the coils is applied and the profile is measured again. The difference between these two measurements, normalized to the correction value, gives the response function of the coil (Fig. 5). We assume that all corrections are small and the response functions have a linear dependence on these corrections. Assuming that the response functions are the same for all coils the compensating field is modeled (1).

$$B(\vec{a},z)=\sum_j a_j f(z-\xi_j) \tag{1}$$

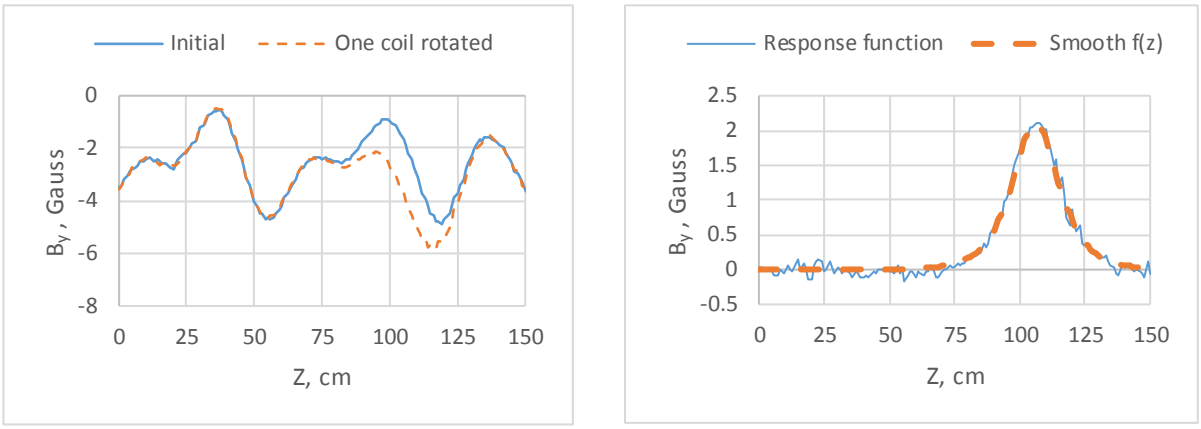

(a) (b)

Fig. 5: Measurements of the coil response function

Values of the corrections can be calculated using the least squares method.

$$L(\vec{a})=\sum_i \left(b_i - B(\vec{a},z_i)\right)^2 + g\cdot\sum_j a_j^2 \quad \rightarrow \quad \min, \tag{2}$$

where $f(z)$ is the response function of the coil, a_j is the value of the coil correction, b_i and z_i are values of the transverse magnetic field and the coordinates of the measurement location, g is the coefficient limiting the area of influence of each individual coil. $g = 0$ corresponds to the case when each coil affects unlimited area and the corrections with no limitation become too large (Fig. 6). However, if $g > 0$ the constructed field compensates the magnetic profile incompletely, and the procedure has to be iterated several times.

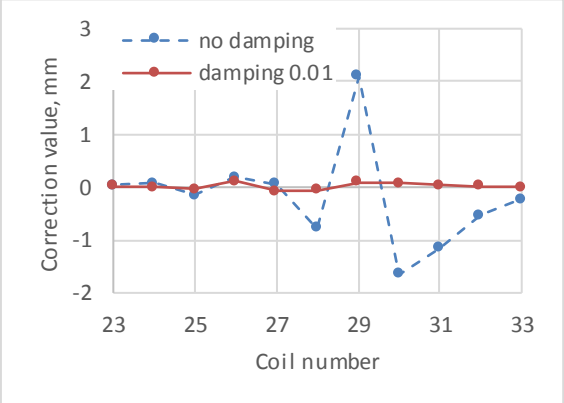

Fig. 6: Correction values for different given damping coefficients

After several iterations of applying corrections to the solenoid coils, the straightness of the magnetic field in the cooling section reached $4\square 10^{-5}$ *rad* (Fig. 7). Nevertheless, it is not enough to adjust the coils of the main solenoid only once. During experiments with electron cooling the operational fields of the cooling system can change, thus the magnetization of those elements changes. Since the efficiency of the electron cooling strongly depends on the quality of the magnetic field, the changing magnetization must be compensated in real time. The scheme of compensation of the magnetization is discussed in the next section.

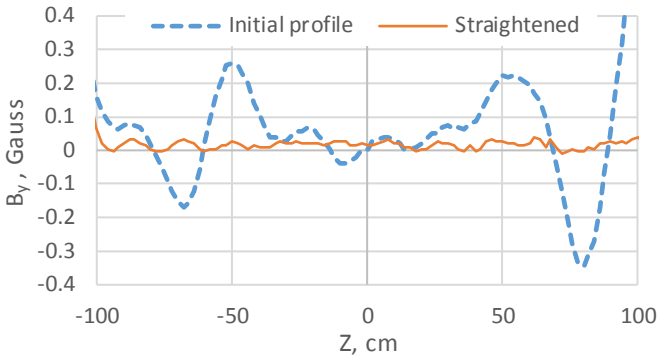

Fig. 7: Profiles of the vertical magnetic field in the cooling section

4 Magnetization

Magnetization of the magnetic elements contributes to the transversal magnetic field and depends on operational magnetic fields. In this section, the number of presented operational regimes is reduced, because the goal is to demonstrate the methodology rather than display all the results. The list of discussed operational regimes is presented in Table 1.

Table 1: Operational regimes used in measurements and corresponding operational currents of magnetic elements.

Regime name	Supply current of magnetic elements		
	Main solenoid	Bending magnets and vertical solenoids	Dipoles
Regime 1	167.4 A	500 A	221.2 A
Regime 2	134.4 A	400 A	178 A
Regime 3	100 A	300 A	132.7 A

The first well-known problem due to magnetization is non-repeatability of magnetic profiles (Fig .8). However, this problem has a well known solution called cycling, which consists of ramping the magnets down and up to reduce hysteresis effects. To achieve repeatability, the cycling is applied every time the operational regime is changed, and thus, for the same regimes we get the same profile curves while the shape of curves related to different regimes can differ (Fig. 9).

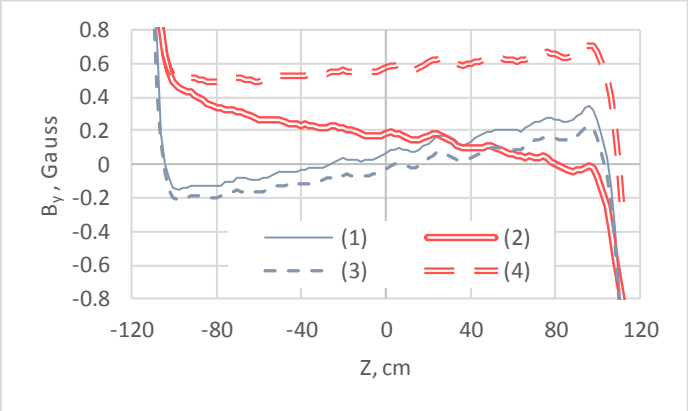

Fig. 8: Non-repeatability of measurements. Curves (1) and (3) correspond to Regime 2, (2) and (4) to Regime 3. Regimes were changed in the following order: from (1) to (2) without cycling, then to (3) and then to (4) with cycling. States (2) and (4) both correspond to Regime 3, but the profiles are different.

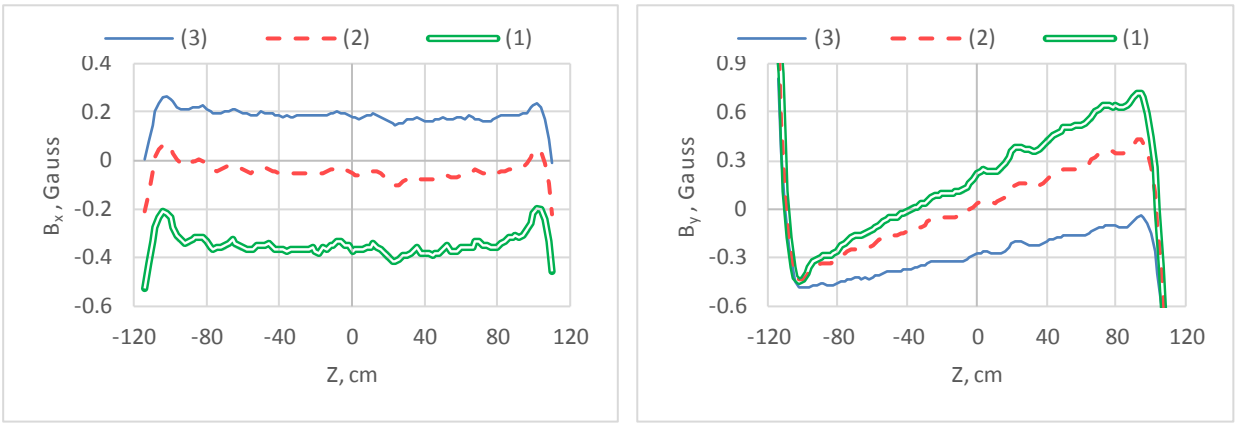

(a) (b)

Fig. 9: Magnetic profiles at different operational regimes. (a) shows horizontal profiles, (b) shows vertical profiles. States 1,2 and 3 represent regime numbers which are described in Table 1.

For simplicity we assume that the longitudinal component of the magnetic field in the cooling section depends only on the operational current of the main solenoid. Now we can take into account the displacement of the measured profile curves. In Section 2, we noted that the optical axis of the compass feedback system is aligned with the magnetic axis of the main solenoid. If there is a tilt between these two axes, the longitudinal field contributes to the measured value of the transversal field (Fig. 10). The contribution is proportional to the longitudinal field, so it can be calculated by comparing several measurements at different operational regimes and then be excluded from further consideration.

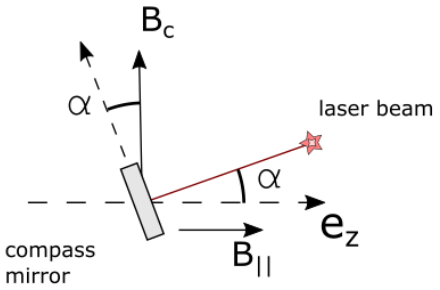

Fig. 10: Systematic measurement error due to the tilt between the optical axis and the axis of the main solenoid. $B_C^* = B_{||} \sin\alpha$, where α is a tilt value, $B_{||}$ is the longitudinal magnetic field strength, B_C^* is an addition to the measured transverse component of the magnetic field.

Another issue is the slope of the magnetic profile changing with operational current (Fig. 9(b) and Fig. 11(a)). During magnetic measurements made at BINP the magnetic field strength in the cooling section was varied from 400 Gauss to 1 kGauss. Changing operational currents in all magnetic elements proportionally (with respect to the operational current of the bending magnets), the slope of the magnetic fields changes linearly with the operational current (Fig. 11(b)). Such profiles are compensated by special corrections of the coils of the main solenoid. As Figure 12 shows, as a result of such corrections, the slope of the magnetic field does not depend on the operational current anymore.

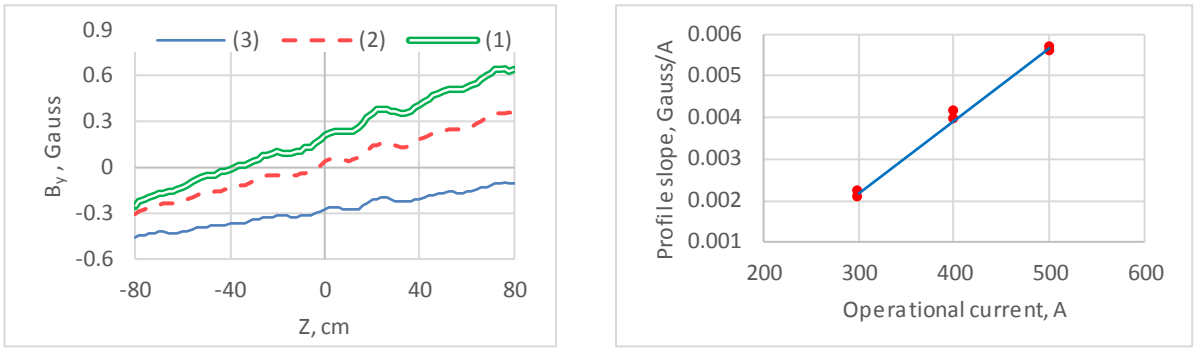

(a) (b)

Fig. 11: Slope of the profile of the vertical magnetic field. Graph (a) is the profile limited by boundaries of the cooling site. Graph (b) demonstrates that if the operational currents are changed proportionally, the slope behaves according to a linear function of the operational current.

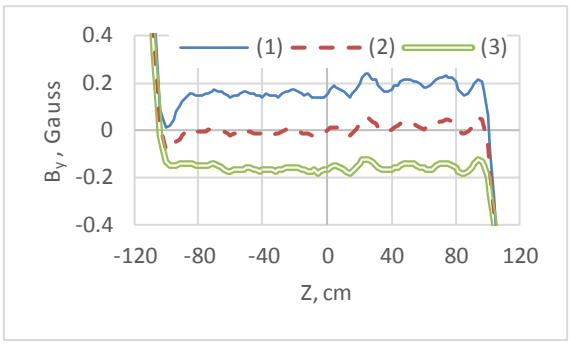

Fig. 12: By changing the operational current proportionally, a special correction to the coils of the main solenoid is applied, such that the shape of the vertical profile doesn't depend on the operational current.

The last question is how the magnetic profile changes, when the operational current is changed only in one symmetrical pair of the magnetic elements. In this case the measurements are similar to the previous ones. One varies only one operational current, measures the profiles and calculates the normalized difference, called the magnetization response function of the magnetic element. As shown in Fig. 13, the magnetization response function slightly depends on the operational current while the shape of the response function in the cooling section can be considered as constant. The total magnetization response is expected to be a linear function of all operational current deviations $\Delta B_y = k_1 \cdot \Delta I_1 + k_2 \cdot \Delta I_2 + k_3 \cdot \Delta I_3$, where $k_{1,2,3}$ are magnetization response functions of different pairs of elements.

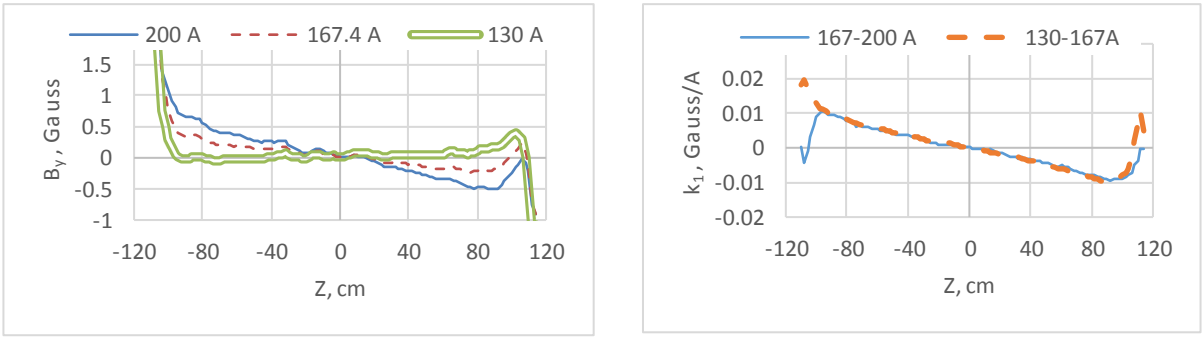

(a) (b)

Fig. 13: Measurements of the magnetization response function of the main solenoid. (a) shows series of measurements, (b) shows the magnetization response functions for different combinations of the main solenoid operational current.

To prove this concept, we compared the measured profile curves and the curves calculated by Eq. (3) (Fig. 14(a)).

$$B_i = B_0 + k_1 \cdot \Delta I_1^i + k_2 \cdot \Delta I_2^i + k_3 \cdot \Delta I_3^i, \tag{3}$$

where B_0 is the original magnetic profile corresponding to regime 1, $\Delta I_{1,2,3}^i$ are deviations of operational currents of i-th regime from the currents corresponding to regime 1.

Going further one can say that the operational currents are just deviations from the zero-state corresponding to the residual magnetization. As a result, one can obtain the profile of the residual magnetization by simply subtracting the modelled curves of profiles from the measured ones using Eq. (4) (Fig. 14(b)).

$$B_i^{res} = B_i^{meas} - k_1 \cdot I_1^i - k_2 \cdot I_2^i - k_3 \cdot I_3^i \tag{4}$$

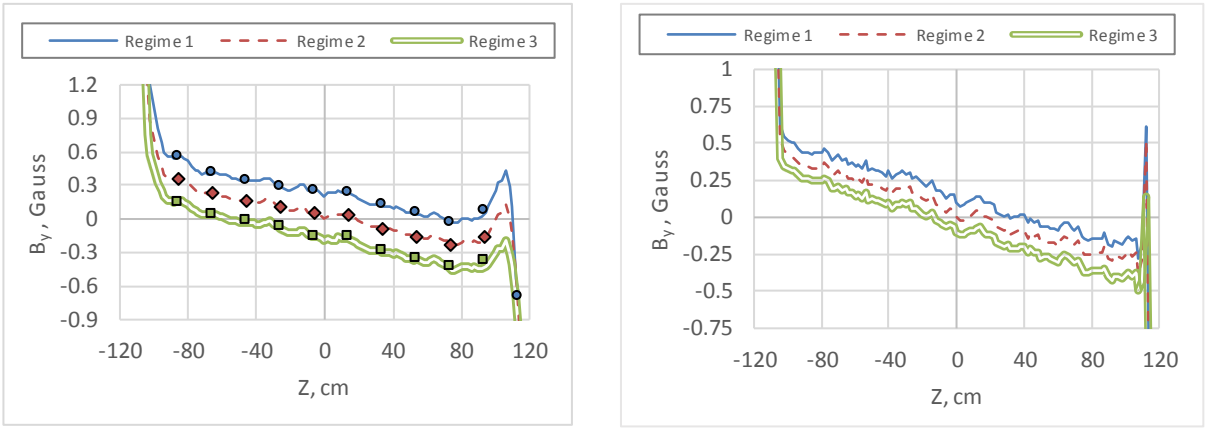

(a) (b)

Fig. 14: Using magnetization response functions to recover the profile of the residual magnetization. (a) shows comparison of modelled and measured profiles, (b) shows calculated profiles of the residual magnetization. Presented curves are separated artificially.

As expected from the previous results, the residual magnetization does not depend on the operational currents.

With information about the residual magnetization and the magnetization response functions of magnetic elements one can predict changes of the magnetic profiles resulting from changes in operational magnetic regimes. Thus, such changes can be compensated by the magnetic correctors of the cooling section.

5 First experiments with an electron beam

Before disassembling the electron cooler and sending it to JINR (Dubna) we performed several experiments with an electron beam at an energy 6 keV. The most interesting parameters are the perveance of the cathode and the current losses (Fig. 15). After one week of cathode training, the electron beam DC current reached 500 mA and the current losses were less than 1 μA. As Fig. 15(b) shows, initially current losses increase with increasing beam current. However, at some point a beam space charge creates a potential barrier near the suppressor that locks the secondary emission from the collector.

The subsequent increase of the beam current can lead to the opposite effect. If the potential barrier is too high and the electron beam is not able to reach the collector, in most cases the beam will die on the walls of vacuum chambers. In other words, it results in a rapid increase of current losses.

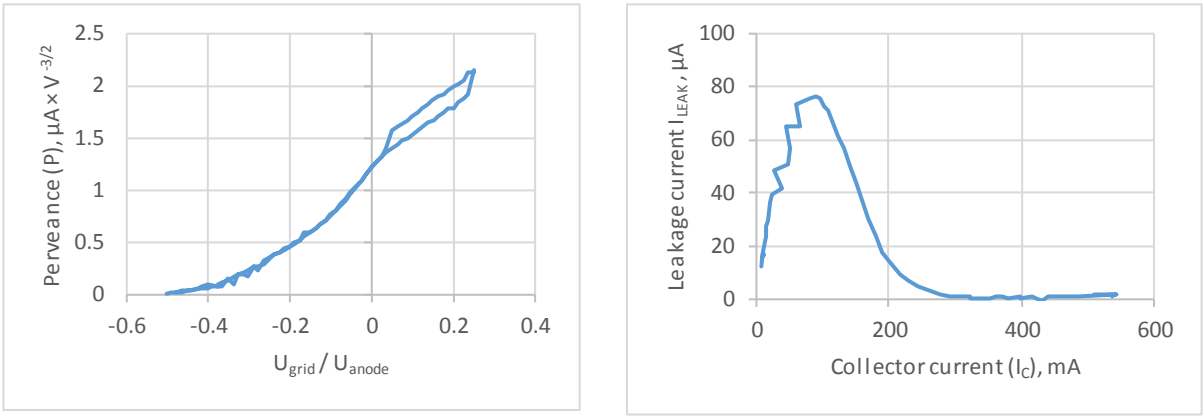

(a) (b)

Fig. 15: Measurements of the perveance of the electron gun (a) and the electron beam current losses (b)

6 Conclusion

For efficient electron cooling it is vital to have high quality magnetic fields in the cooling section of the electron cooler system. This article covers basic aspects of measuring the magnetic fields and controlling the shape of the magnetic profile in the cooling section. However, obtained results are applicable for an operational field strength equal to or less than 1 kGauss. After the electron cooler is sent to JINR (Dubna), we will conduct further experiments with magnetic field strengths up to 2 kGauss and electron beam currents up to 3 A at an energy of 60 keV.

References

[1] NICA – Nuclotron-based Ion Collider facility. Retrieved from http://nica.jinr.ru.

[2] V.V. Parkhomchuk and A.N. Skrinski, Electron cooling: 35 years of development, Uspekhi Fizicheskikh Nauk, Russian Academy of Science (2000)